

## Electromechanical Fields in Piezoelectric Semiconductor Nanofibers under an Axial Force

C.L. Zhang<sup>1,2,3,\*</sup>, Y.X. Luo<sup>1</sup>, R.R. Cheng<sup>1</sup> and X.Y. Wang<sup>1</sup>

<sup>1</sup>Department of Engineering Mechanics, Zhejiang University, Hangzhou, 310027, China

<sup>2</sup>Soft Matter Research Center (SMRC), Zhejiang University, Hangzhou, 310027, China

<sup>3</sup>Key Laboratory of Soft Machines and Smart Devices of Zhejiang Province, Hangzhou, 310027, China

### ABSTRACT

Piezoelectric semiconductor (PS) nanofibers, which simultaneously exhibit piezoelectricity and unique electric conductive behavior, have huge applications in sensors, energy harvesters, and piezoelectric field effect transistors. Electromechanical fields and charge carrier in PS nanofibers can be effectively controlled by a mechanical force. One-dimensional linear equations for PS nanofibers, which are suitable for small axial force and small electron concentration perturbation, are presented. Analytical expressions for the electromechanical fields and electron concentration in the fiber are obtained. Numerical results show that the electromechanical fields near the two ends are sensitive to the initial electron concentration and the applied axial force.

### INTRODUCTION

Piezoelectric semiconductor (PS) materials and structures have found wide range applications in multi-functional electronic devices due to the unique synergy of piezoelectric and semiconducting properties [1]. The interaction between the piezoelectric potential and the charge carrier in PS materials and structures under a bias voltage or mechanical force, makes them exhibit a variety of novel mechanical, electronic, and optical behaviors. Relatively recently, various one-dimensional (1D) PS nanostructures have been synthesized, such as ZnO fibers, tubes, belts and spirals [2-4]. They can be made into single structures [5-8] or in arrays [9-12], and have been used to make energy harvesters for converting mechanical energy into electrical energy [13-17], piezoelectric field effect transistors [2, 3, 18] operated by mechanical fields, acoustic charge transport devices [19], and strain, gas, humidity and chemical sensors [2, 20].

A mechanical force can be utilized to effectively control and tune the properties of PS structures. For example, the external strain-induced piezoelectric potential can be as a ‘gate’ voltage [1], and can be used to improve the performance of optoelectronic devices [6]. It is important to theoretically comprehend the electromechanical behaviors of 1D PS structures under external stimuli for their applications in devices. There are many experimental and modeling investigations on 1D PS structures in the above-mentioned references. However, studies based on analytical models of PS structures are still very limited. By using the perturbation method, Gao and Wang first derived the analytical formula for electrostatic potential in a bent ZnO nanowire pushed by a lateral force; however, they neglected the effect of piezoelectric field on the mechanical deformation of the ZnO nanowire [21]. That is to say, the analytical model developed in [21] is semi-coupled, not a fully coupled one. Professor Z. L. Wang and his co-authors systematically investigated, with the finite element method, the coupled piezoelectric and semiconductive behavior of a ZnO wire under lateral bending [5] and compression [15]. Quasi-1D ZnO nanowires under axial stress were theoretically studied using fully coupled non-linear FEM calculations by Araneo et al.[7], who eventually found that quasi-1D piezo-semiconductor structures

with floating electrodes could achieve maximum piezopotential and conversion efficiency, in open-circuit condition. An accurate theoretical model can be very helpful to understand precisely the mechanical and electric behaviors of PS structures, which is the key to design PS devices with an optimized performance. We develop a fully coupled analytical model for one-dimensional PS structures in [22] very recently. The basic behaviors of piezoelectric semiconductors are described by the conventional phenomenological theory [23] consisting of the equations of linear piezoelectricity [24] and the equations of the conservations of charge of electrons and holes [25]. The anisotropy of piezoelectric materials, the electromechanical couplings in them, and the nonlinearity associated with the drift currents of electrons and holes which are proportional to the products of the unknown carrier densities and the unknown electric field, make theoretical analyses of piezoelectric semiconductor devices difficult. The analytical model in our previous paper [22] is linearized under the assumption of small axial force and hence small carrier concentration perturbations from the reference state. In this paper, we investigate the mechanical and electric behaviors of a fixed-free ZnO PS fiber under an axial force at the free end using the linear analytical model. The effect of the axial force and carrier concentration on the electromechanical fields in the PS fiber is thoroughly studied. It should be noted that ZnO fibers used in devices at present are at the nanoscale. Various small-scale effects, such as surface effect, flexoelectricity, and polarization gradient etc., may have an effect on the mechanical and electrical properties of ZnO nano-fibers, which however will not be considered here.



Figure 1. A piezoelectric semiconductor fiber under an axial force  $F$

## THEORETICAL FORMULATIONS

Consider an n-type piezoelectric semiconductor fiber made of ZnO as shown in Figure 1. The length of the fiber is  $2l$ , the shape of the cross section  $A$  may be arbitrary. The fiber is assumed to be long and thin, i.e., its length is much larger than the characteristic dimension of the cross section. For example, if the fiber is cylindrical in shape with the diameter being  $d$ , we assume that the fiber is sufficiently long and thin such that  $1 \ll l/d$ . The  $c$ -axis of the ZnO crystal is along the axis of the fiber, i.e., the  $x_3$  axis. The lateral surface of the fiber is traction free. It is fixed at  $x_3 = -l$ . The fiber is under the action of axial force  $F$  at  $x_3 = l$ , which produces an axial stress  $T = F/A$ . The classical infinitesimal deformation theory is adopted in this paper.

The deformation of the fiber under the axial force is mainly an axial extension. For simplicity, one-dimensional model is employed here. Hence, there are the axial displacement  $u_3$ , the axial stress  $T_3$ , the axial electric displacement  $D_3$ , and the axial electric current  $J_3^n$ . From (25), the equilibrium equation, electrostatic equation, and continuity equation for PS 1D fibers are, respectively,

$$\frac{\partial T_3}{\partial x_3} = 0, \quad \frac{\partial D_3}{\partial x_3} = q(N_D^+ - n), \quad \frac{\partial J_3^n}{\partial x_3} = 0, \quad (1)$$

where  $q$  is the magnitude of the elementary electronic charge,  $n$  the concentration of electrons,  $N_D^+$  the concentration of impurities of donors which are assumed to be uniform along the fiber.

Note: carrier recombination and generation is neglected in equation (1). In addition, the effect of the stress on the energy bands is not considered in this paper. From [22], the axial force, electric displacement, and electric current in PS fibers can be written as,

$$T_3 = \bar{c}_{33}S_3 - \bar{e}_{33}E_3, D_3 = \bar{e}_{33}S_3 + \bar{\epsilon}_{33}E_3, J_3^n = qn\mu_{33}^n E_3 + qD_{33}^n \frac{\partial n}{\partial x_3}, \quad (2)$$

where  $\mu_{33}^n$  and  $D_{33}^n$  are the mobility and diffusion constants of the electron, respectively. The effective material constants are  $\bar{c}_{33} = 1/s_{33}$ ,  $\bar{e}_{33} = d_{33}/s_{33}$  and  $\bar{\epsilon}_{33} = \epsilon_{33} - d_{33}^2/s_{33}$ . Here,  $s_{33}$ ,  $d_{33}$  and  $\epsilon_{33}$  are the compliance, piezoelectric, and dielectric constants[24]. The axial strain and the axial electric field in equation (2) are  $S_3 = \frac{\partial u_3}{\partial x_3}$  and  $E_3 = -\frac{\partial \phi}{\partial x_3}$ , respectively.

The ZnO fiber considered here is assumed to be the uniformly doped semiconductor with  $N_D^+$ . The electron current in equation (2)<sub>3</sub> includes the nonlinear term of the product of carrier concentration and electric field, which makes it difficult to get the analytical solution. Here, we employ a linearized method proposed in [22]. We assume that the carrier concentration  $n_F$  in the nanofiber after being applied the small axial force  $F$ , has a small perturbation  $n_1$  at its equilibrium state  $n_0$ . Namely, the electron concentration in the nanofiber can be written as  $n_F = n_0 + n_1$ . For the uniformly doped case, there is a relation of  $n_0 = N_D^+$ . As a result, the electrostatic equation in equation (1)<sub>2</sub> and the electron density in equation (2)<sub>3</sub> become

$$D_{3,3} = -qn_1, \quad J_3^n = qn_0\mu_{33}^n E_3 + qD_{33}^n \frac{\partial n_1}{\partial x_3}. \quad (3)$$

The governing equations in equation (1) can be written as

$$\bar{c}_{33} \frac{\partial^2 u_3}{\partial x_3^2} + \bar{e}_{33} \frac{\partial^2 \phi}{\partial x_3^2} = 0, \quad \bar{e}_{33} \frac{\partial^2 u_3}{\partial x_3^2} - \bar{\epsilon}_{33} \frac{\partial^2 \phi}{\partial x_3^2} = qn_1, \quad -qn_0\mu_{33}^n \frac{\partial^2 \phi}{\partial x_3^2} + qD_{33}^n \frac{\partial^2 n_1}{\partial x_3^2} = 0. \quad (4)$$

### Electromechanical Fields in the Fiber under a constant force

The electromechanical fields in the fiber under the axial force  $F$ , for given mechanical and electric boundary conditions, can be obtained in a systematic and straightforward manner. The mechanical boundary conditions are  $T_3(l) = T$  and  $u_3(-l) = 0$ . We consider the electrical boundary conditions of  $\phi(-l) = 0$ ,  $D_3(l) = 0$  and  $J_3^n(\pm l) = 0$ . The global charge neutrality condition of  $\int_{-l}^l n_1 dx_3 = 0$  should be satisfied as well. With the above boundary conditions, from equation (4), we can easily obtain the analytical solutions of electromechanical fields in the fiber, they are

$$\begin{aligned} u_3 &= \frac{T}{\bar{c}_{33}} \left[ -\frac{k_{33}^2}{1+k_{33}^2} \frac{1}{\kappa} \left( \frac{\sinh \kappa x_3}{\cosh \kappa l} + \tanh \kappa l \right) + x_3 + l \right], \\ \phi &= \frac{Tk_{33}^2}{\bar{e}_{33}(1+k_{33}^2)\kappa} \left( \frac{\sinh \kappa x_3}{\cosh \kappa l} + \tanh \kappa l \right), \quad E_3 = \frac{Tk_{33}^2}{\bar{e}_{33}(1+k_{33}^2)} \frac{\cosh \kappa x_3}{\cosh \kappa l}, \\ n_1 &= \frac{T\bar{e}_{33}\kappa}{\bar{c}_{33}q} \frac{\sinh \kappa x_3}{\cosh \kappa l}, \quad D_3 = \frac{T\bar{e}_{33}}{\bar{c}_{33}} \left( 1 - \frac{\cosh \kappa x_3}{\cosh \kappa l} \right), \end{aligned} \quad (4)$$

where  $k_{33}^2 = \bar{\epsilon}_{33}\bar{\epsilon}_{33} / \bar{\epsilon}_{33}\bar{\epsilon}_{33}$ ,  $\kappa^2 = qn_0\mu_{33} / \bar{\epsilon}_{33}(1+k_{33}^2)D_{33}$ . Obviously, when  $n_0$  approaches to zero,  $\kappa$  is close to zero, the fields in equation (4) for a PS fiber are degenerated into for a pure piezoelectric fiber.

## NUMERICAL RESULTS

As a numerical example, consider the n-type ZnO fiber with the total length  $2l=1.2\mu\text{m}$ , the radius is  $100\text{nm}$ . In the following calculations, the compliance, piezoelectric, and dielectric constants [26] are  $S_{33}=6.94\times 10^{-12}\text{ N/m}^2$ ,  $d_{33}=11.67\times 10^{-12}\text{ C/N}$ ,  $\epsilon_{33}=1.12\times 10^{-10}\text{ F/m}$ . We investigate the effect of the axial force on the electromechanical fields in the fiber. The initial carrier concentration is assumed to be  $8\times 10^{22}\text{m}^{-3}$ . For different axial forces  $F$  (10nN, 15nN and 20nN), we use equation (4) to calculate  $n_1$ ,  $n_1/n_0$ ,  $\phi$ ,  $E_3$ ,  $u_3$ ,  $D_3$  in the fiber, respectively, and plot them in figures 2-4. It can be seen that the carrier perturbation  $n_1$ , electric potential, and electric displacement vary more rapidly near the ends of the fiber than in the central part. As the axial force  $F$  increases, all fields become stronger. All the fields except for the axial displacement change greatly within  $0.1\mu\text{m}$  near the two ends of the fiber for different axial forces. The axial displacement in figure 4 is linearly dependent of the axial position in the fiber, which shows that the axial displacement is dominated by the linear term. From figure 2, the value of  $n_1/n_0$  is from  $-0.04$  to  $0.04$ , which indicates the carrier perturbation  $n_1$  is far smaller than  $n_0$ . This shows that the linear model is valid, and hence numerical results are correct in this paper.

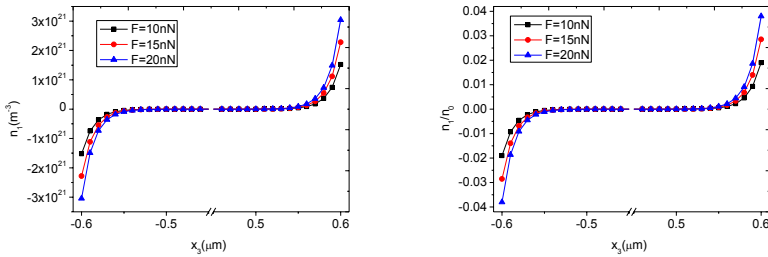


**Figure 2.** Axial distributions of  $n_1$  (left) and  $n_1/n_0$  (right) for different values of axial force  $F$ .

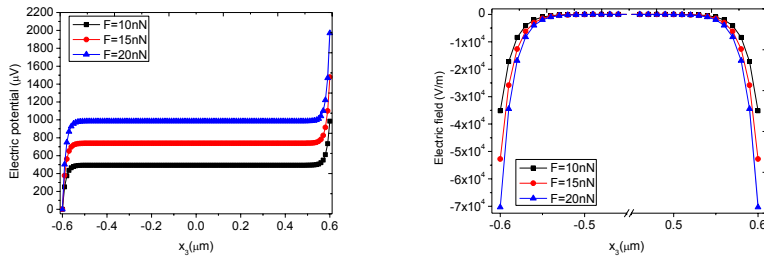


**Figure 3.** Axial distributions of electric potential  $\phi$  (left) and electric field  $E_3$  (right) for different values of axial force  $F$ .

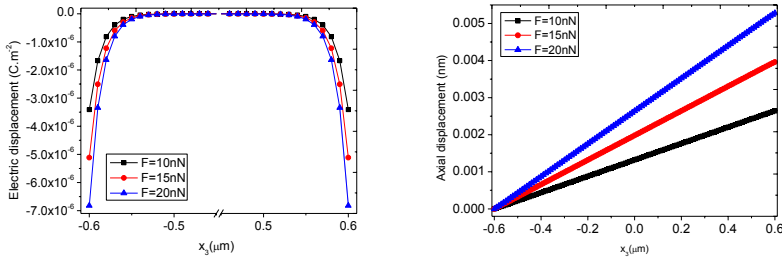


**Figure 4.** Axial distributions of electric displacement  $D_3$  (left) and axial displacement  $u_3$  (right) for different values of axial force  $F$ .

To investigate the effect of  $n_0$  on the electromechanical fields in the fiber, we fix the axial force  $F=10nN$ , and calculate  $n_1/n_0$  and  $\phi$  for different values of  $n_0$  ( $2 \times 10^{22} m^{-3}$ ,  $4 \times 10^{22} m^{-3}$  and  $8 \times 10^{22} m^{-3}$ ). The curves of  $n_1/n_0$  and  $\phi$  versus the axial position of the fiber are plotted in figure 5. Similarly, the values of  $n_1/n_0$  and electric potential  $\phi$  vary rapidly near the two ends of the fiber. As the initial carrier concentration of  $n_0$  increases, both  $n_1/n_0$  and  $\phi$  decrease. The value of  $\kappa$  varies with the value of  $n_0$ , as a result, the regions of rapid variation for the electric potential and  $n_1/n_0$  are different for different  $n_0$ .

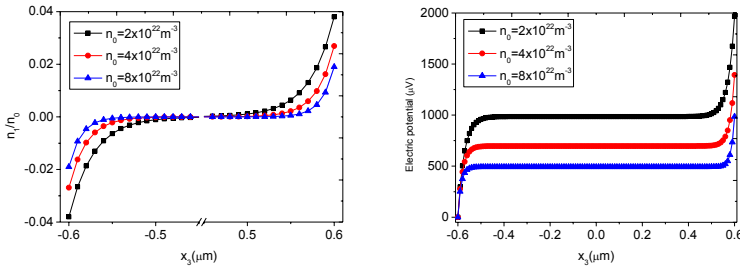


**Figure 5.** Axial distributions of  $n_1/n_0$  (left) and  $\phi$  (right) for different values of  $n_0$ .

## CONCLUSIONS

One-dimensional linear equations are presented for the axial extension of a piezoelectric semiconductor fiber. The model is simple and valid for small loads and small carrier concentration perturbations. Within the linear model, the analytical expressions of the electromechanical fields and the carrier concentrations in the PS fiber under an axial force are

obtained. All the electromechanical fields except for the axial displacement vary rapidly near the two ends of the fiber.

## ACKNOWLEDGMENTS

This work was supported by the National Natural Science Foundation of China (Nos. 11672265, 11202182, 11272281 and 11321202), and the Fundamental Research Funds for the Central Universities (Nos. 2016QNA4026 and 2016XZZX001-05).

## REFERENCES

- [1] Z.L. Wang, *Adv. Mater.* **24**, 4632 (2012).
- [2] Z.L. Wang, *Adv. Mater.* **15**, 432 (2003).
- [3] Z.L. Wang, *Nano Today* **5**, 540 (2010).
- [4] B. Kumar and S.W. Kim, *J. Mater. Chem.* **21**, 18946 (2011).
- [5] Y.F. Gao and Z.L. Wang, *Nano Lett.* **9**, 1103 (2009).
- [6] Y.F. Hu, Y.L. Chang, P. Fei, R.L. Snyder and Z.L. Wang, *ACS Nano* **4**, 1234 (2010).
- [7] R. Araneo, G. Lovat, P. Burghignoli and C. Falconi, *Adv. Mater.* **24**, 4719 (2012).
- [8] J.L. Ji, Z.Y. Zhou, X. Yang, W.D. Zhang, S.B. Sang and P.W. Li, *Small* **9**, 3014 (2013).
- [9] Y. Shen, J. Hong, S. Xu, S.S. Lin, H. Fang, S. Zhang, Y. Ding, R.L. Snyder and Z.L. Wang, *Adv. Funct. Mater.* **20**, 703 (2010).
- [10] Chen T T, Cheng C L, Fu S P and Chen Y F 2007 Photoelastic effect in ZnO nanorods *Nanotech.* **18**, 225705.
- [11] J. Yoo, C.H. Lee, Y.J. Doh, H.S. Jung and G.C. Yi, *Appl. Phys. Lett.* **94**, 223117 (2009).
- [12] H.Z. Xue, N. Pan, M. Li, Y.K. Wu, X.P. Wang and J.G. Hou, *Nanotech.* **21**, 215701 (2010).
- [13] P.X. Gao, J.H. Song, J. Liu and Z.L. Wang, *Adv. Mater.* **19**, 67 (2007).
- [14] M.Y. Choi, D. Choi, M.J. Jin, I. Kim, S.H. Kim, J.Y. Choi, S.Y. Lee, J.M. Kim and S.W. Kim, *Adv. Mater.* **21**, 2185 (2009).
- [15] G. Romano, G. Mantini, A.D. Garlo, A. D'Amico, C. Falconi and Z.L. Wang, *Nanotech.* **22**, 465401 (2011).
- [16] A. Asthana, H.A. Ardakani, Y.K. Yap and R.S. Yassar, *J. Mater. Chem. C* **2**, 3995 (2014).
- [17] Q.L. Liao, Z. Zhang, X.H. Zhang, M. Mohr, Y. Zhang and H.J. Fecht, *Nano Res.* **7**, 917 (2014).
- [18] X.D. Wang, J. Zhou, J.H. Song, J. Liu, N.S. Xu and Z.L. Wang, *Nano Lett.* **6**, 2768 (2006).
- [19] S. Buyukkose, A. Hernandez-Minguez, B. Vratzov, C. Somaschini, L. Geelhaar, H. Riechert, W.G. van der Wiel and P.V. Santos, *Nanotech.* **25**, 135204 (2014).
- [20] J. Yu, S.J. Ippolito, W. Wlodarski, M. Strano and K. Kalantar-Zadeh, *Nanotech.* **21**, 265502 (2010).
- [21] Y.F. Gao and Z.L. Wang, *Nano Lett.* **7**, 2499-2505 (2007).
- [22] C.L. Zhang, X.Y. Wang, W.Q. Chen and J.S. Yang, *Smart Mater. Struct.* **26**, 025030 (2017)
- [23] A.R. Hutson and D.L. White, *J. Appl. Phys.* **33**, 40 (1962).
- [24] B.A. Auld, *Acoustic Fields and Waves in Solids*, Vol. I, John Wiley and Sons, New York, 1973.
- [25] R.F. Pierret, *Semiconductor Fundamentals*, 2<sup>nd</sup> ed., Addison-Wesley, Reading, Massachusetts, 1988.
- [26] Z.L. Wang, R. Yang, J. Zhou, Y. Qin, C. Xu, Y. Hu and S. Xu, *Mater. Sci. Eng. R: Rep.* **70**, 320 (2010).